Available online at www.sciencedirect.com
ScienceDirect
Solar Energy 84 (2010) 685–690
SOLAR ENERGY
www.elsevier.com/locate/solener

A new code for the design and analysis of the heliostat field layout for power tower system

Xiudong Wei [a], Zhenwu Lu [a,*], Weixing Yu [a], Zhifeng Wang [b]

[a] Changchun Institute of Optics, Fine Mechanics and Physics of Chinese Academy of Sciences, Changchun 130033, China
[b] The Key Laboratory of Solar Thermal Energy and Photovoltaic system, Institute of Electrical Engineering, Chinese Academy of Sciences, Beijing 100190, China

Received 8 June 2009; received in revised form 18 January 2010; accepted 24 January 2010
Available online 18 February 2010

Communicated by: Associated Editor L. Vant-Hul

Abstract

A new code for the design and analysis of the heliostat field layout for power tower system is developed. In the new code, a new method for the heliostat field layout is proposed based on the edge ray principle of nonimaging optics. The heliostat field boundary is constrained by the tower height, the receiver tilt angle and size and the heliostat efficiency factor which is the product of the annual cosine efficiency and the annual atmospheric transmission efficiency. With the new method, the heliostat can be placed with a higher efficiency and a faster response speed of the design and optimization can be obtained. A new module for the analysis of the aspherical heliostat is created in the new code. A new toroidal heliostat field is designed and analyzed by using the new code. Compared with the spherical heliostat, the solar image radius of the field is reduced by about 30% by using the toroidal heliostat if the mirror shape and the tracking are ideal. In addition, to maximize the utilization of land, suitable crops can be considered to be planted under heliostats. To evaluate the feasibility of the crop growth, a method for calculating the annual distribution of sunshine duration on the land surface is developed as well.

Keywords: Power tower system; Heliostat field; Nonimaging optics; Aspherical heliostat; Edge ray principle

1. Introduction

In the power tower systems, the lower dense solar radiation is concentrated and reflected by heliostat field onto a receiver atop tower, and then in the receiver the very dense solar power is translated into thermal power to generate electricity. The heliostat field is a very important subsystem because it contributes about 50% (Kolb et al., 2007) to the total cost of system and its annual energy loss is about 47% (William and Micheal, 2001). The codes such as DELSOL3, HFLCAL, WinDELSOL1.0, SENSOL (Garcia et al., 2008; Annual Report, 2001; Relloso and Domingo, 2005) and so on have been developed for the design and optimization of the heliostat field layout. There are some shortcomings in the current design of the heliostat field layout. Firstly, the field boundary is normally constrained by the extended angle, the tower height and the receiver size (Siala and Elayeb, 2001; Dellin et al., 1986). Although this definition of the field boundary is simple, it is difficult to obtain a higher efficiency for the heliostat layout. Sanchez (Sanchez and Romero, 2006) presented a method for the design of heliostat layout based on yearly normalized energy surfaces, but the iterative calculation of the annual efficiency of heliostat during the design and optimization results in a very low response speed. In addition, the layout pattern is not regular and it is difficult to optimize the receiver tilt angle and size as well as the tower height. Secondly, the spherical heliostat dominates current power tower system. However, spherical heliostat suffers from large spillage

* Corresponding author.
E-mail address: luzhenwu55@yahoo.com.cn (Z. Lu).

0038-092X/$ - see front matter © 2010 Elsevier Ltd. All rights reserved.
doi:10.1016/j.solener.2010.01.020

losses due to the serious aberrations (Igel and Hughes, 1979; Zaibel et al., 1995). Therefore, a new aspherical heliostat with corrected aberration needs to be developed to increase the optical efficiency of the heliostat field. Thirdly, the utilization of the land under heliostats is not considered in current heliostat layout design. The solar power tower system occupies a very large area of land like PS10 and PS20 in Spain. To maximize the utilization of land, suitable crops, e.g. sweet potato, should be considered to be planted on the land under heliostats. Therefore, the annual sunshine duration on the land surface under heliostats needs to be analyzed.

In this work, a new code for the design and analysis of heliostat field layout is developed by employing the MATLAB software. A new method for the heliostat field layout design is proposed in order to improve the response speed of the design and optimization of heliostat field. For analyzing performance of the aspherical heliostats, a new module is created in the new code. To evaluate the feasibility of planting crops on the field land under heliostats, a new calculation method for the annual sunshine duration is developed as well.

2. A new method for the heliostat field layout design

The annual performance of the heliostat field depends on the cosine loss, the mirror reflectance loss, the atmospheric attenuation loss, the blocking & shadowing loss and the receiver spillage loss (William and Micheal, 2001). The annual cosine loss is the largest loss term which contributes to about 23.4% of the total field loss. Following the cosine effect, the atmospheric attenuation loss is about 6%. The blocking & shadowing loss and the receiver spillage loss are about 5.6% and 2%, respectively. These losses can be suppressed through proper field design. The mirror reflectance loss is about 10% and has nothing to do with the field configuration. In order to make sure the heliostats are placed with lower cosine, spillage and atmospheric attenuation losses, the field boundary needs to be constrained by the tower height, the receiver tilt angle and size as well as the heliostat efficiency factor. The flow chart of the new method of heliostat layout design is shown in Fig. 1.

The instantaneous cosine efficiency of a heliostat based on the cosine loss equals to the cosine of incident angle θ relative to the heliostat center which can be calculated by the formula (7) in reference Wei et al. (2007). By averaging the integration of the instantaneous cosine efficiency over a year, the annual cosine efficiency can be obtained. The atmospheric transmission efficiency based on the atmospheric attenuation loss strongly depends on the weather condition and the distance between the heliostat and the receiver. For a visual distance of about 40 km, the atmospheric transmission efficiency can be calculated simply by the formula (4) in reference Schmitz et al. (2006). The heliostat efficiency factor equals to the product of the annual cosine efficiency and the annual atmospheric transmission efficiency.

The field boundary should also be constrained by the tower height and the receiver tilt angle and size to reduce the spillage loss. The receiver aperture normally has a circular or rectangular shape, therefore its projection boundary on the field land is an ellipse or trapezium as shown in Fig. 2.

For the circular aperture, the equation of the elliptical boundary can be easily derived as follows,

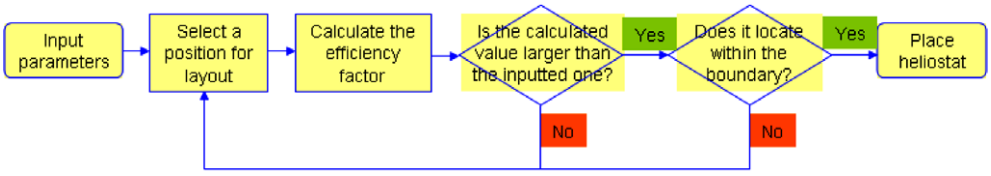

Fig. 1. Flow chart of the heliostat layout design with the new method.

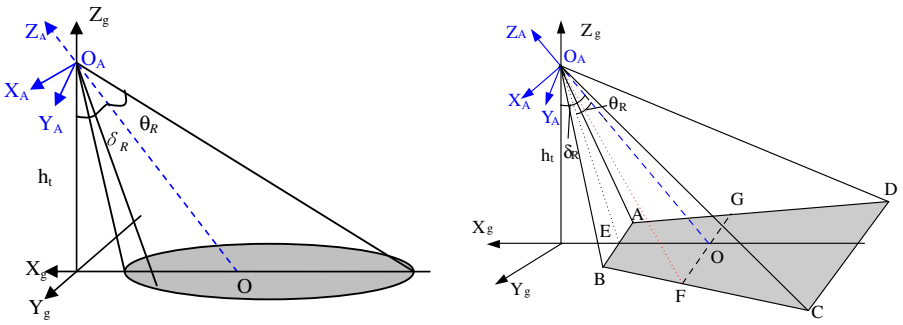

(a) Circular aperture projection (b) Rectangular aperture projection

Fig. 2. Projection boundary on the field land from receiver aperture.

$$y^2 + (\cos\delta_R x + \sin\delta_R h_t)^2 - \tan^2\theta_R(\sin\delta_R x - \cos\delta_R h_t)^2 = 0 \quad (1)$$

For the rectangular aperture, the coordinate of the vertex A of the trapezoidal boundary can be derived according to the geometrical relationship shown in Fig. 3.

$$\begin{cases} x_A = \frac{h_t(\tan\theta_R\cos\delta_R - \sin\delta_R)}{\cos\delta_R + \tan\theta_R\sin\delta_R} \\ y_A = \frac{-\tan\theta_R h_t}{\cos\delta_R + \tan\theta_R\sin\delta_R} \end{cases} \quad (2)$$

where h_t is the tower height, δ_R is the tilt of the receiver, θ_R is the receiving angle of the receiver. The coordinates of vertexes B, C and D can be calculated by using the same method.

The definition of the receiving angle is similar to the accepting angle of compound parabolic concentrator in the nonimaging optics (Winston et al., 2005). According to the geometrical relationship shown in Fig. 4, the formula for calculating the receiving angle has been derived as follows,

$$\sin\theta_R = \frac{-2dl + L\sqrt{4l^2 + L^2 - d^2}}{4l^2 + L^2} \quad (3)$$

where d is the diameter of the reflected spot in heliostat field, D is the size of the receiver aperture ($D \geqslant d$), L is the diameter of the absorbing aperture ($L \geqslant D$), l is the distance between the receiver aperture and the absorbing aperture.

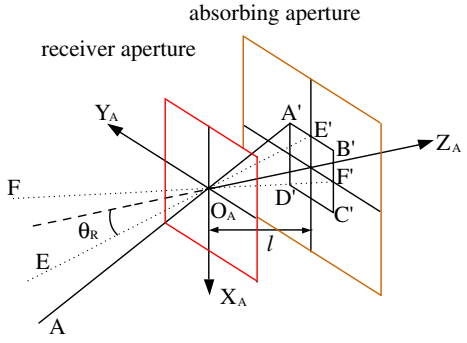

Fig. 3. Assistant figure for solving the coordinate of the vertex A.

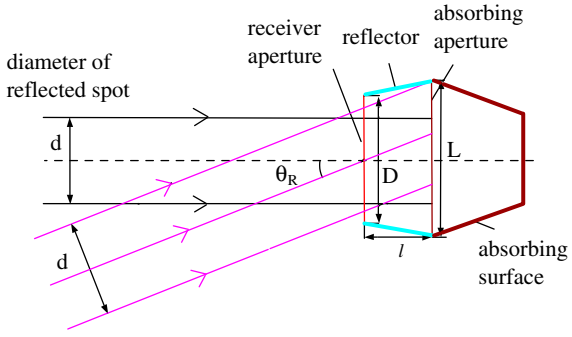

Fig. 4. Definition of accepting angle of the cavity receiver.

The system efficiency also strongly depends on the blocking and shadowing efficiency which depends on the distance between heliostats and the heliostats arrangement. The blocking and shadowing efficiency can be calculated by ray tracing. The calculation details were presented in reference (Wei et al., 2007). To reduce the spacing, the distance between heliostats needs to be optimized by using the parametric search algorithm (Wei et al., 2007). The merit function can be written as follows,

$$F_{merit} = \frac{1}{\rho \cdot \eta} \quad (4)$$

where ρ is the heliostat density which depends on the spacing, η is the annual field efficiency which is the product of the annual cosine efficiency, the annual shadowing and blocking efficiency, the annual interception efficiency, the annual atmospheric transmission efficiency and the mirror reflection efficiency. By using the merit function, the field configuration with higher heliostat density and higher annual field efficiency can be obtained after the optimization.

The categories of heliostats arrangement include radial cornfields, radial staggers, N–S cornfields and N–S staggers (Lipps and Vant-Hull, 1978). For every category a relative optimal field configuration can be selected after optimization. Finally the radial stagger configuration is chosen as an optimal field layout.

Based on the new method, a new code for the design of the heliostat field layout has been developed. The accuracy and feasibility of the code has been confirmed by comparing with the published data of current PS10 field (Yao et al., 2009). A new layout for the PS10 plant at the PS10 location has been designed by using the new code. The PS10 field (10 MW Solar Thermal Power Plant, 2006; Annual Report, 2003; PS10, 2005) consists of 624 heliostats in an area of $12.84 \times 9.45\ m^2$ and located at 37.4° North Latitude. The heliostat positions can be obtained according to the figure on page 5 of reference (PS10, 2005). The reflectivity of mirror is set to be about 0.88. The receiver is a cavity with a rectangular aperture of 13.78 m × 12 m. The tilt angle of the receiver is 12.5°. The tower height is 100.5 m. The initial configuration parameters of the new layout are the same as the PS10 except the receiver tilt angle and the heliostats position. The designed optimal tilt angle of the receiver for the new layout is 17°. The new layout pattern is shown in Fig. 5, where the color map denotes the distribution of the heliostat efficiency factor on the field land, the blue dotted line denotes the constraint boundary defined by the tower height and the rectangular receiver tilt and receiving angle. As can be seen from the figure that the blue dots are quite far away from the heliostats, which means that all the heliostats could have an interception efficiency of 100% in theory, this is because the receiving angle of receiver is calculated from the Eq. (3) based on the constant solar image of heliostat field. In practice, the mirror shape errors and the tracking errors will result in a larger solar image whose size changes with the solar radiation time continuously and thus causes some spillage loss. The system annual optical effi-

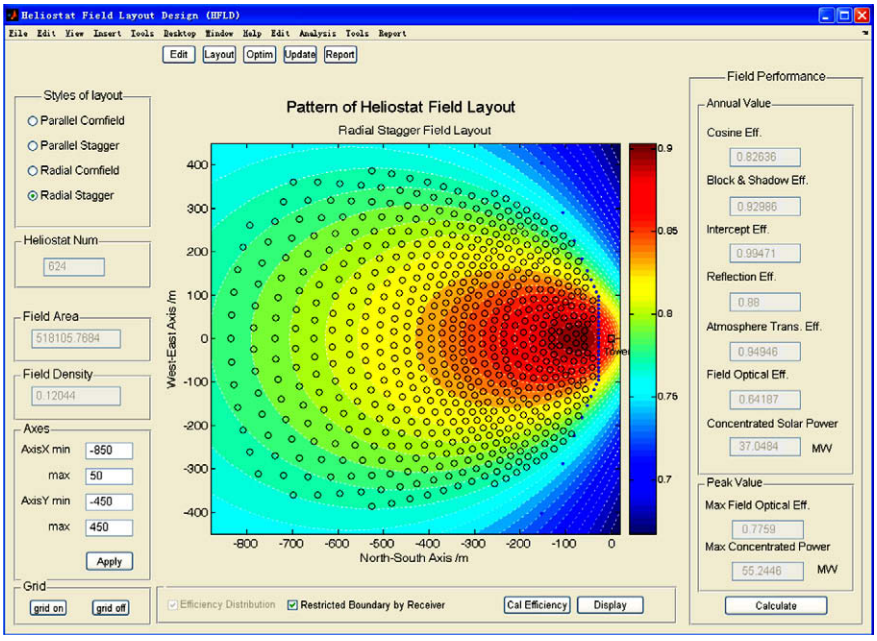

Fig. 5. A new heliostat field for the PS10 plant designed by using the new method.

ciency of the new field layout is 64.19%, which agrees well with that of current PS10 layout. Therefore, the new method is proved to be feasible for the design of heliostat field layout.

It should be noted that the heliostat can be placed with higher interception efficiency without needing to calculate the annual spillage loss of heliostat for the new method. A single computation of the annual interception efficiency of heliostat field is sufficient when estimating the performance of the field configuration during the optimization. Therefore, the new code has a higher response speed in terms of the shorter computing time during the design and optimization of the heliostat field.

3. A software module for the analysis of aspherical heliostat

The aspherical heliostat requires that the incident plane of sunlight coincide with the meridian plane of the heliostat during the tracking. The target aligned mount meets this requirement (Ries and Shubnell, 1990). The mathematical models for the aspherical heliostat field have been created by using the Monte Carlo ray tracing method. A new field for 1 MW power tower system has been designed by using the new code as shown in Fig. 6. The field consists of 110 heliostats in an area of $11 \times 11\ m^2$ and located at 40.4° North Latitude. The tower has a height of 81.5 m. The tilt angle of the receiver is 28°. The target aligned mount is used in the heliostats.

The daily maximum radius of solar image generated by both aspherical toroidal heliostats and spherical heliostats for the field layout of Fig. 6 has been calculated as shown in Fig. 7. It can be seen that the annual maximum geometrical and root mean square radius of solar image of toroidal heliostat field are just 3.5 and 1.0 m, respectively, whereas for

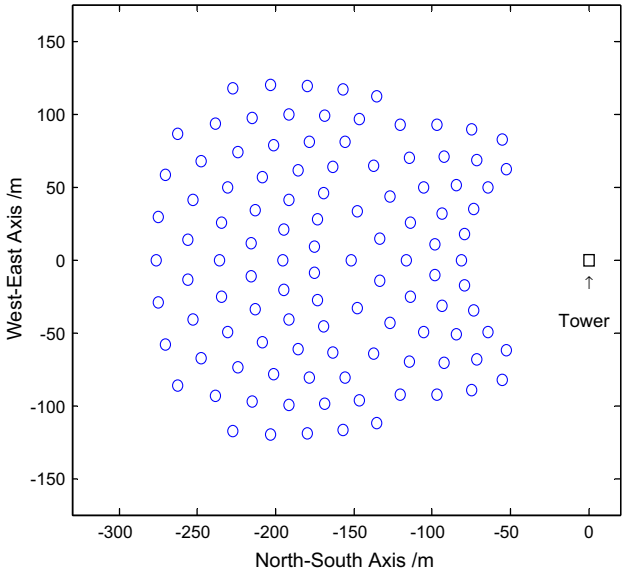

Fig. 6. Pattern of heliostat field for 1 MW power tower system.

spherical heliostat field these values are 5.6 and 1.4 m, respectively. Therefore, the geometrical radius of solar image has been reduced by about 30% by using the toroidal heliostats and thus a higher total efficiency or concentration ratio of the power tower system can be obtained by using the toroidal heliostats.

4. Calculation of the sunshine duration on the land surface

The equation of the incident ray from the sun passing the heliostat surface can be written as follows,

$$\frac{x - x_m}{\cos A \cos \alpha} = \frac{y - y_m}{\sin A \cos \alpha} = \frac{z - z_m}{\sin \alpha} \tag{5}$$

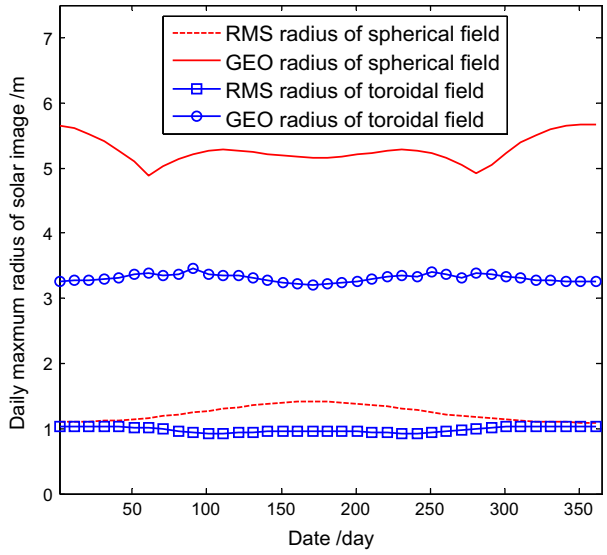

Fig. 7. Daily maximum radius of the solar image as a function of the days over a year for spherical and aspherical heliostat field, where GEO radius denotes the geometrical radius of the solar image and RMS radius denotes the root mean square radius of the solar image.

where (x_m, y_m, z_m) is the coordinate of a heliostat surface in the ground coordinate system, α is the solar altitude angle (William and Micheal, 2001), A is the solar azimuth angle (William and Micheal, 2001). The coordinate of the intersection point between the land surface $z = 0$ and the incident ray can be easily solved as follows,

$$\begin{aligned} x &= x_m - z_m ctg\alpha \cos A \\ y &= y_m - z_m ctg\alpha \sin A \end{aligned} \tag{6}$$

The calculation procedure for the sunshine duration on the land surface is shown in Fig. 8.

If the total sample number of time is u and the element value corresponding to the facet of land surface in matrix $\mathbf{B}'$ is v, the duration of sunshine on the land facet can be calculated by the following formula,

$$T_{shine} = T\frac{v}{u} \tag{7}$$

where T is the duration of sunshine without heliostats.

Taking the PS10 field as an example, the distribution of sunshine duration on the land surface under heliostats is calculated by the new code and is shown in Fig. 9. The observed period is from the 81st day to the 265th day of a year. In the map, the blue areas represent short duration of sunshine which is not suitable for planting crops, and the red areas represent long duration of sunshine which can be considered for planting suitable crops.

There are a few issues need to be addressed for farming under heliostats including the use of the farming equipment without damaging the heliostat, leaving enough space for cleaning vehicles between the heliostats and allowing enough sunlight to reach the ground so that the crop can grow and so on. Here we propose some suggestions which should be helpful for these issues. Firstly, suitable crops need to be selected to ensure that the crop can grow under the heliostat according to the distribution map of the sunshine duration on field land. Secondly, the self-cleaning coatings (Liu et al., 2008; Omer et al., 2009) can be applied onto the surface of the solar reflector to eliminate the use of the cleaning vehicles. Thirdly, the farming equipment can be used because the distance between the large heliostats is about 20 m. Finally, the heliostat surface should be able to be rotated to make room for the farming equipment. Moreover, it is worth to point out that the frequency of the use of the farming equipment and the machine for heliostat maintenance is just a few times, which will further lower the cost to maintain the heliostat field. By considering all above, to plant crops under heliostat seems

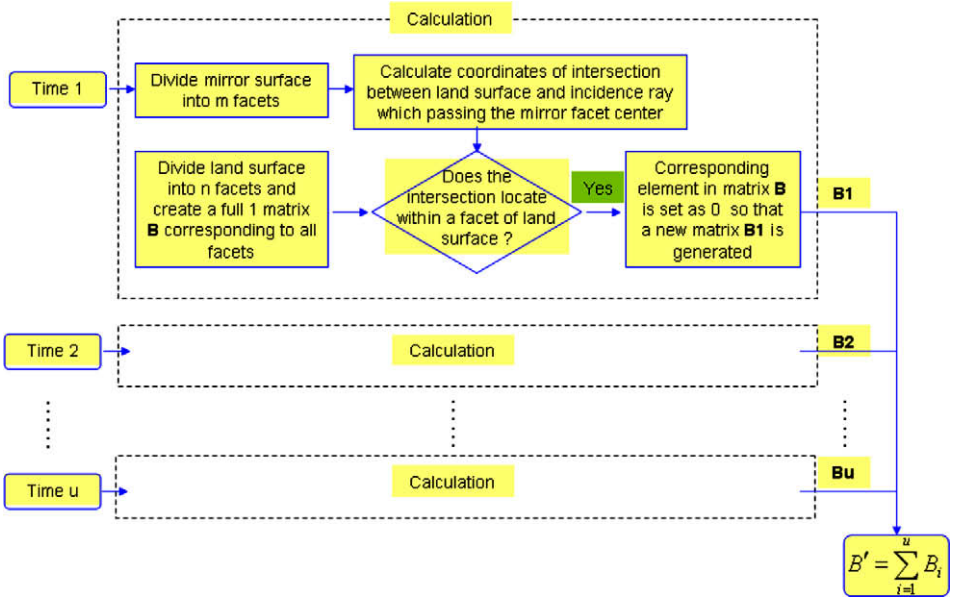

Fig. 8. The flow chart of calculation of sunshine duration on the land surface.

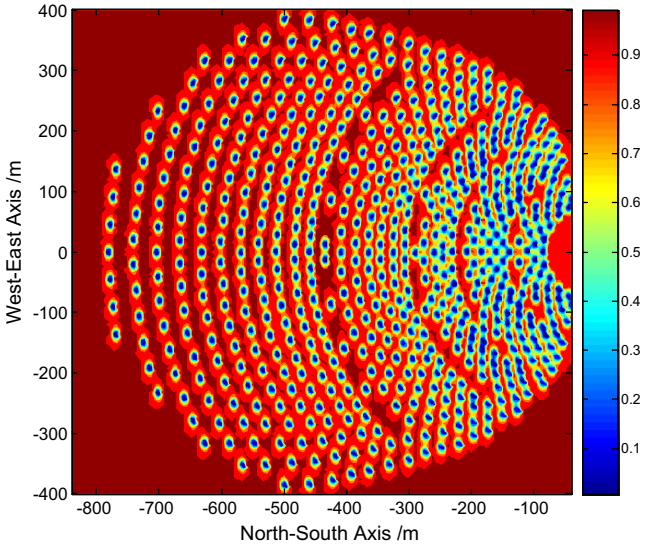

Fig. 9. Distribution map of the sunshine duration of the PS10 field land.

very promising and can maximize the utilization of the land source further.

5. Conclusions

In this work, a new code for design and analysis of the heliostat field layout is presented. A new method to constrain the boundary of the field layout has been proposed. With the new method, the heliostats can be placed with a higher optical efficiency and the computing process is much faster due to the elimination of the iterative calculation of the annual interception efficiency in traditional method. A new layout for the PS10 plant has been designed by using the new code. The system annual efficiency of the new field layout is as good as that of current PS10 layout. Therefore, the new method is proved to be feasible. A new module for the analysis of the aspherical heliostats is created in the new code and by which a new toroidal heliostat field layout is analyzed. It was found that the toroidal heliostat field has a higher performance than the spherical heliostat field if the mirror shape and the tracking are ideal. Finally, in order to increase the utilization of field land, a new calculation method for annual distribution of sunshine duration is presented and some useful suggestions have been proposed to make the idea of planting crops under heliostat more promising and feasible.

Acknowledgements

The authors acknowledge the financial support from the National High Technology Research and Development Program of China (Grant # 2006AA050101, 2006AA050103) and the National Basic Research Program of China (Grant # 2010CB227101).

References

10 MW Solar Thermal Power Plant for Southern Spain, 2006. Available from: <http://ec.europa.eu/energy/res/sectors/doc/csp/ps10_final_report.pdf>.

Annual Report 2001 of PSA, 2001. Available from: <http://www.psa.es/webeng/techrep/2001/atr2001eng.pdf>.

Annual Report 2003 of PSA, 2003. Available from: <http://ww.psa.es/webeng/techrep/2003/ATR2003_ing.pdf>.

Dellin, T.A., Fish, M.J., Yang, C.L., 1986. A user's manual for DELSOL3: a computer code for calculating the optical performance and optimal system design for solar thermal central receiver plants. Sandia National Labs Report SAND86-8018.

Garcia, P., Ferriere, A., Bezian, J.J., 2008. Codes for solar flux calculation dedicated to central receiver system applications: a comparative review. Solar Energy 82, 189–197.

Igel, E.A., Hughes, R.L., 1979. Optical analysis of solar facility heliostats. Solar Energy 22, 283–295.

Kolb, G.J., Jones, S.A., Donnelly, M.W., et al., 2007. Heliostat cost reduction study, SAND 2007-3293. Available from: <http://www.prod.sandia.gov/cgi-bin/techlib/access-control.pl/2007/073293.pdf>.

Lipps, F.W., Vant-Hull, L.L., 1978. A cell wise method for the optimization of large central receiver systems. Solar Energy 20, 505–516.

Liu, Zhaoyue, Zhang, Xintong, Murakami, Taketoshi, et al., 2008. Sol–gel SiO_2/TiO_2 bilayer films with self-cleaning and antireflection properties. Solar Energy Materials and Solar Cells 92, 1434–1438.

Kesmez, Omer, Erdem Camurlu, H., Burunkaya, Esin, et al., 2009. Sol–gel preparation and characterization of anti-reflective and self-cleaning SiO_2–TiO_2 double-layer nanometric films. Solar Energy Materials and Solar Cells 93, 1833–1839.

PS10: a 11.0 MW Solar Tower Power Plant with Saturated Steam Receiver, 2005. Available from: <http://www.upcomillas.es/catedras/crm/report05/Comunicaciones/Mesa%20IV/D%20Valerio%20Fern%C3%A1ndez%20-%20Solucar%202.pdf>.

Relloso, S., Domingo, M., 2005. Solar projects analysis using SENSOL. Available from: <http://www.sener.es/EPORTAL_DOCS/GENERAL/FILE-cw0bd117fad3d64a6e9638/SOLARPROJECTSANALYSISUSINGSENSOL.pdf>.

Ries, H., Shubnell, M., 1990. The optics of a two-stage solar furnace. Solar Energy Materials 21 (2–3), 213–217.

Sanchez, M., Romero, M., 2006. Methodology for generation of heliostat field layout in central receiver systems based on yearly normalized energy surfaces. Solar Energy 80, 861–874.

Schmitz, M., Schwarzbozl, P., Buck, R., 2006. Assessment of the potential improvement due to multiple apertures in central receiver systems with secondary concentrators. Solar Energy 80, 111–120.

Siala, F.M.F., Elayeb, M.E., 2001. Mathematical formulation of a graphical method for a no-blocking heliostat field layout. Renewable Energy 23, 77–92.

Wei, X.D., Lu, Z.W., Lin, Z., 2007. Optimization procedure for design of heliostat field layout of a 1MWe solar tower thermal power plant. Proceeding of SPIE 6841, 684119-1–684119-10.

William, B.S., Micheal, G., 2001. Power from the sun. Available from: <http://www.powerfromthesun.net/book.htm>.

Winston, R., Minano, J.C., Benitez, P., 2005. Nonimaging Optics. Elsevier Academic Press.

Yao Zhihao, Wang Zhifeng, Lu Zhenwu, Wei Xiudong, 2009. Modeling and simulation of the pioneer 1 MW solar thermal central receiver system in China. Renewable Energy 34, 2437–2446.

Zaibel, R., Dagan, E., Karni, J., et al., 1995. An astigmatic corrected target-aligned heliostat for high concentration. Solar Energy Material and Solar Cells 37 (2), 191–202.